Automatica 129 (2021) 109697

Contents lists available at ScienceDirect

Automatica

journal homepage: www.elsevier.com/locate/automatica

Brief paper

Network-based deployment of nonlinear multi agents over open curves: A PDE approach☆

Maria Terushkin, Emilia Fridman *

School of Electrical Engineering, Tel Aviv University, Israel

ARTICLE INFO

Article history:
Received 6 October 2020
Received in revised form 28 January 2021
Accepted 5 April 2021
Available online xxxx

Keywords:
Distributed parameter systems
Multi-agent systems
Network-based control
Time-delay

ABSTRACT

Deployment of the first-order and second-order nonlinear multi agent systems over desired open (and, as a particular case, closed) smooth curves in 2D or 3D space is considered. The considered nonlinearities are globally Lipschitz. We assume that the agents have access to the local information of the desired curve and to their positions with respect to their closest neighbors (as well as to their velocities for the second-order systems), whereas in addition a leader agent is able to measure its absolute position. We assume that a small number of leaders (distributed in the spatial domain) transmit their measurements to other agents through a communication network. We take into account the following network imperfections: variable sampling, transmission delay and quantization. We propose a static output-feedback controller and model the resulting closed-loop system as a disturbed (due to quantization) nonlinear heat equation (for the first-order systems) or damped wave equation (for the second-order systems) with delayed point state measurements, where the state is the relative position of the agents with respect to the desired curve. In order to cope with the open curve we consider Neumann boundary conditions that ensure mobility of the boundary agents. We derive linear matrix inequalities (LMIs) that guarantee the input-to-state stability (ISS) of the system. The advantage of our approach is in the simplicity of the control law and the conditions. Numerical examples illustrate the efficiency of the method.

1. Introduction

Deployment of a large-scale multi agent system (MAS), where a group of agents rearrange their positions into a target spatial configuration in order to achieve a common goal, has recently attracted attention of many researchers, e.g. Mesbahi and Egerstedt (2010) and Oh, Park, and Ahn (2015). This is due to vast applications, such as cooperative movement of robots or vehicles (Ren, Beard, & Atkins, 2007), biochemical reaction networks, animal flocking behavior (see Olfati-Saber, 2006), search-and-rescue, environmental sensing and monitoring (Dunbabin & Marques, 2012), etc. The majority of the existing works in the field of MAS is concentrated on deploying of interconnected agents, modeled by ordinary differential equations (ODEs) that provide efficient methods when the number of agents is low.

When the number of agents is large, a methodology based on partial differential equations (PDEs) becomes efficient. In Frihauf and Krstic (2010) and Meurer (2012), the agents were treated as a continuum, and the collective dynamics was modeled by a reaction–diffusion PDE, under the boundary control. Feedforward control combined with backstepping-based boundary controller was implemented in Freudenthaler and Meurer (2020), where the collective dynamics was modeled by a modified viscous Burger's equation. Finite-time deployment formations along predefined spatiotemporal paths by means of boundary control were contemplated in Meurer and Krstic (2011). The problem of driving the state of a network of agents, modeled by boundary controlled heat equations, toward a common steady state profile was addressed in Pilloni, Pisano, Orlov, and Usai (2015). Formation tracking problem using complex-valued PDE with an input-to-state stability (ISS) type of convergence was considered in Jie, Feng, and Jinpeng (2015). Formation tracking control of a MAS, where the collective dynamics was modeled by a wave PDE was studied in Tang, Qi, and Zhang (2017). Control of collective dynamics of a large-scale MAS moving in a 3D space under the occurrence of an arbitrarily large boundary input delay was

☆ Supported by Israel Science Foundation (grant no. 673/19), by C. and H. Manderman Chair at Tel Aviv University, Israel and by Y. and C. Weinstein Research Institute for Signal Processing, Israel. The material in this paper was partially presented at the 21st IFAC World Congress (IFAC 2020), July 12-17, 2020, Berlin, Germany. This paper was recommended for publication in revised form by Associate Editor Thomas Meurer under the direction of Editor Miroslav Krstic.

* Corresponding author.
E-mail addresses: mariater@mail.tau.ac.il (M. Terushkin), emilia@tauex.tau.ac.il (E. Fridman).

https://doi.org/10.1016/j.automatica.2021.109697
0005-1098/

considered in Qi, Wang, Fang, and Diagne (2019). All the above methods employ boundary control of linear PDEs.

In the case of measurements of the leaders' absolute positions, the majority of PDE-based results employ the PDE observer for output-feedback control. The latter may be difficult for implementation. Recently a simple static output-feedback controller was suggested in Wei, Fridman, and Johansson (2019), where it was proposed to transmit the leader's absolute positions with respect to the desired curve to all the agents by using communication network. The network-based results of Wei et al. (2019) were confined to the first-order integrators and to deployment onto the closed curves. Among the network imperfections, the quantization effects were neglected. Moreover, in the case of several leaders a common delay (i.e. synchronized transmissions in the same time with the same network-induced delay) was considered, which may be restrictive. As most of the PDE-based results, Wei et al. (2019) considered linear models of agents.

In this paper we study deployment of the first and second-order nonlinear multi agent systems onto open curves. We assume that the agents have access to their target position on the desired curve and their positions with respect to their closest neighbors, whereas a small number of leaders is able to measure their absolute position with respect to the desired curve. For the second-order MAS all agents measure their velocities. As in Wei et al. (2019), our design is based on spatial decomposition method introduced in Fridman and Blighovsky (2012) for stabilization of semilinear heat equations. For the globally Lipschitz in the state nonlinearities (as considered in the present paper), the spatial decomposition method leads to global stabilization. We propose to transmit the leaders' absolute positions to other agents by using a communication network. However, leaders may use independent networks and their transmissions are not synchronous, which leads to multiple delays in the closed-loop system. Moreover, we take into account the quantization effect (see Liberzon, 2003).

By applying the time-delay approach to networked control systems (see Chapter 7 of Fridman, 2014), we model the resulting closed-loop systems as a disturbed (due to quantization) nonlinear heat equation (for the first-order MAS) and damped wave equation (for the second-order MAS) with the delayed point state measurements. In order to cope with open target curves we consider Neumann boundary conditions that ensure mobility of the boundary agents. Neumann boundary conditions are also applicable to the closed curves. Note that the existing results on spatial decomposition under the point delayed measurements are confined to a single delay and unperturbed systems (see Fridman & Blighovsky, 2012; Kang & Fridman, 2019; Terushkin & Fridman, 2019). In this paper, we introduce delayed input-to-state stabilization via spatial decomposition under the point measurements, where ISS analysis of the closed-loop system is based on combination of the Lyapunov–Krasovskii method with the generalized Halanay's inequality (Wen, Yu, & Wang, 2008). Moreover, the case of multiple delays is treated. We derive LMI conditions that guarantee ISS. The advantage of our approach is in the simplicity of the control law and conditions. Numerical examples of deployment onto smooth open and closed curves in 3D illustrate the efficiency of the method. Some preliminary results confined to the second-order MAS have been presented in Terushkin and Fridman (2020b).

Notation. Throughout the paper the notation $P > 0$ with $P \in \mathbb{R}^{n\times n}$ means that P is symmetric and positive definite. The symmetric elements of a symmetric matrix will be denoted by $*$. Functions, continuous (continuously differentiable) in all arguments, are referred to as of class C (of class C^1). $L^2(0,L)$ is the Hilbert space of square integrable functions $z(\xi)$, $\xi \in [0,L]$ with the corresponding norm $\|z\|^2_{L^2} = \int_0^L z^2(\xi)d\xi$. $\mathcal{H}^1(0,L)$ is the Sobolev space of absolutely continuous scalar functions $z : [0,L] \to \mathbb{R}$ such that $z' \in L^2(0,L)$ with the norm $\|z\|^2_{\mathcal{H}_1} = \|z\|^2_{L^2} + \|z'\|^2_{L^2}$. $\mathcal{H}^2(0,L)$ is the Sobolev space of scalar functions $z : [0,L] \to \mathbb{R}$ with absolutely continuous z' and with $z'' \in L^2(0,L)$.

1.1. Mathematical preliminaries

The following inequalities will be useful:

Lemma 1.1 (*Wirtinger's Inequality Fridman & Blighovsky, 2012*)**.** *Let $z \in \mathcal{H}^1[a,b]$ be a scalar function with $z(a) = 0$ or $z(b) = 0$. Then*

$$\int_a^b z^2(\xi)d\xi \le 4\frac{(b-a)^2}{\pi^2}\int_a^b [z'(\xi)]^2 d\xi \tag{1.1}$$

Lemma 1.2 (*Sobolev's Inequality Kang & Fridman, 2019*)**.** *Let $z(x) \in \mathcal{H}^1(0,L)$ be a scalar function. Then, for all $C > 0$*

$$\max_{x\in[0,L]} z^2(x) \le (L+C)\int_0^L z^2(\xi)d\xi + \frac{1}{C}\int_0^L [z'(\xi)]^2 d\xi. \tag{1.2}$$

Lemma 1.3 (*Generalized Halanay's Inequality Wen et al., 2008*)**.** *Let $V : [t_0-\tau_M, \infty) \longrightarrow \mathbb{R}^+$ be absolutely continuous function, and $w : [t_0,\infty) \longrightarrow \mathbb{R}$ be a bounded continuous function satisfying $|w(t)| \le \Delta_w$ for all $t \ge t_0$, where $\Delta_w > 0$ is given. If there exists $0 < \alpha_1 < \alpha_0$ and γ^2 such that*

$$\dot V(t) + 2\alpha_0 V(t) - 2\alpha_1 \sup_{-\tau_M\le\theta\le 0} V(t+\theta) - \gamma^2|w(t)|^2 \le 0$$

holds almost for all $t \ge t_0$, then

$$V(t) \le \exp\big(-2\alpha(t-t_0)\big)\sup_{-\tau_M\le\theta\le 0} V(t_0+\theta) + \frac{\gamma^2}{\varepsilon}\Delta_w^2,\ t \ge t_0, \tag{1.3}$$

where $\varepsilon = 2(\alpha_0-\alpha_1) > 0$, and $\alpha > 0$ is a unique positive solution of $\alpha = \alpha_0 - \alpha_1\exp(2\alpha\tau_M)$.

2. Deployment of the first-order MAS

2.1. Problem formulation

Consider a group of N agents, governed by the first-order dynamics, that can move in space $\mathbb{R}^n$, $n \in \{2,3\}$. The agents are located on the initial C^1 curve $\Gamma_0 : [0,L] \longrightarrow \mathbb{R}^n$ in the points $\Gamma_0(h), \dots, \Gamma_0(hN)$ with $h = \frac{L}{N}$. Our objective is to deploy the agents onto the desired C^2 curve $\Gamma : [0,L] \longrightarrow \mathbb{R}^n$. If $\Gamma(0) \ne \Gamma(L)$, the curve Γ is open. We assume that the curves Γ_0 and Γ are without intersections. N points are assigned on the desired curve with constant spacing $h = \frac{L}{N}$, namely $\Gamma(h), \dots, \Gamma(hN)$ which will give the final desired position of each agent. For simplicity, we assume that the desired curve does not evolve over time. We neglect collision avoidance as we assume agents of zero volume operating within a large workspace. Furthermore, we assume that no static or moving obstacles are present in the operating workspace.

The dynamics of each agent is given by

$$\begin{aligned}&\dot z_i^j = u_i^j + f^j(z_i,t), \quad j \in \{1,\dots,n\}, \quad n = 2,3,\\ &i = 1,\dots,N, \quad t \ge t_0,\end{aligned} \tag{2.1}$$

where the nonlinearities f^j are of class C^2. Here $z_i^j \in \mathbb{R}$ and u_i^j are components of the position and control for ith agent, respectively. For brevity, the super-script j will be further omitted. We assume that the derivative $f_z(z,t)$ is uniformly bounded by a constant $\rho_1 > 0$:

$$|f_z(z,t)| \le \rho_1, \quad \forall (z,t) \in \mathbb{R}\times[0,L]\times[t_0,\infty). \tag{2.2}$$

The leader-enabled deployment of mobile agents is considered under the following assumptions:

(1) Agents $i = 2, \dots, N-1$ measure their positions with respect to the closest neighbors $i-1, i+1$. They have access to $\Gamma((i-1)h)$, $\Gamma(ih)$ and $\Gamma((i+1)h)$. The boundary agents with $i = 1$ and $i = N$ measure the relative positions of the agents 2 and $N-1$ and have access to $\Gamma(h)$, $\Gamma(2h)$ and $\Gamma((N-1)h)$, $\Gamma(Nh)$ respectively.
(2) No agent can measure its global position z_i except for the leader agents labeled z_{i_m}, $m \in \{1, \dots, M\}$.
(3) The adjacent agents keep their order.

Prior to the deployment procedure, the agents know their desired position on the curve $\Gamma(ih)$ $(i = 1, \dots, N)$ as well as their corresponding closest neighbors desired curve positions (e.g. this data can be sent through the communication network). Our objective is to deploy the agents onto the desired curve Γ by exploiting $M \ll N$ leaders.

2.2. Controller design and heat equation model

We propose a leader–follower displacement-based control, where the position measurements of the leader agents are transmitted through communication network to other agents. Define

$$z_0(t) = z_2(t), \quad z_{N+1}(t) = z_{N-1}(t), \qquad (2.3)$$
$$\Gamma(0) = \Gamma(2h), \quad \Gamma((N+1)h) = \Gamma((N-1)h).$$

We consider the following static output-feedback controller:

$$\begin{aligned} u_i(t) = & \frac{\upsilon^2}{h^2}\left[z_{i+1}(t) - 2z_i(t) + z_{i-1}(t)\right] \\ & - \frac{\upsilon^2}{h^2}\left[\Gamma\big((i+1)h\big) - 2\Gamma\big(ih\big) + \Gamma\big((i-1)h\big)\right] \\ & - f(\Gamma(ih), t) + \bar{u}_i(t), \quad i = 1, \dots, N. \end{aligned} \qquad (2.4)$$

Here $\bar{u}_i$ will be found below as the product of a constant gain $K > 0$ on the corresponding leaders' position measurements.

Denote the error

$$e_i(t) = z_i(t) - \Gamma(ih), \quad i = 0, \dots N+1, \ t \geq t_0.$$

We have

$$\begin{aligned} & f(z_i, t) - f(\Gamma(ih), t) = \rho(e_i, t)e_i(t), \\ & \rho(e_i, t) = \textstyle\int_0^1 f_z\left(\theta e_i + \Gamma(ih), t\right) d\theta, \end{aligned} \qquad (2.5)$$

where due to (2.2)

$$|\rho| \leq \rho_1 \quad \forall (e_i, t) \in \mathbb{R} \times [t_0, \infty). \qquad (2.6)$$

The closed-loop system (2.1), (2.4) has a form:

$$\begin{aligned} \dot{e}_i(t) = & \frac{\upsilon^2}{h^2}\left[e_{i+1}(t) - 2e_i(t) + e_{i-1}(t)\right] \\ & + \rho(e_i, t)e_i(t) + \bar{u}_i(t) \\ & (i = 1, \dots, N). \end{aligned} \qquad (2.7)$$

We further treat the large-scale MAS (2.1) as a continuum with a spatial domain $x \in [0, L]$. Following Fridman and Blighovsky (2012) and Wei et al. (2019), we divide $x \in [0, L]$ into M sampling intervals

$$0 = x_0 < x_1 < \cdots < x_M = L, \qquad (2.8)$$

with the equal length

$$x_m - x_{m-1} = \Delta = \frac{L}{M}, \quad m = 1, \dots, M. \qquad (2.9)$$

We place the leader agent in the middle $\hat{x}_m = 0.5(x_m - x_{m-1})$ of each interval $[x_{m-1}, x_m]$ (see Fig. 1). Note that if in discretization, the number N_m of agents located on $[x_{m-1}, x_m]$ is even, then leader may be located in such a way that it has $0.5N_m - 1$ agents

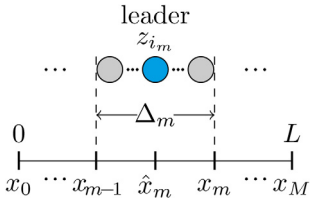

Fig. 1. MAS: leader location.

on $[x_{m-1}, x_m]$ from the left (or right) and $0.5N_m$ from the right (or left).

The leader z_{i_m} sends his absolute (relative to Γ) position $z_{i_m} - \Gamma(i_m h)$ to all the agents z_i located on $[x_{m-1}, x_m)$ through communication network. The measurements are subject to quantization effect, sampling and delays (Fridman & Dambrine, 2009; Liberzon, 2003). A quantizer is a piecewise constant function $q : \mathbb{R} \to \mathbb{R}$ such that

$$|q(y) - y| \leq \Delta_q, \qquad (2.10)$$

where Δ_q is the quantization error bound.

Let $s_0^m < s_1^m < \cdots$ be the sampling times of the measurements with $\lim_{k\to\infty} s_k^m = \infty$ and η_k^m are network-induced delays. We assume that $s_k^m + \eta_k^m < s_{k+1}^m + \eta_{k+1}^m$ for all k. The agents z_i from the interval $[x_{m-1}, x_m]$ employ the controller

$$\begin{aligned} \bar{u}_i(t) = \bar{u}^m(t) = & \quad -Kq(z_{i_m}(s_k^m) - \Gamma(i_m h)) \\ & t \in [s_k^m + \eta_k^m, s_{k+1}^m + \eta_{k+1}^m), \end{aligned} \qquad (2.11)$$

where $\bar{u}_i(t) = 0$ for $t < t_0$. As in Wei et al. (2019), the network-based controller (2.4), (2.11) contains two gains: υ^2 (larger υ^2 allows to reduce the number of the leaders), and K (stabilizes the system and compensates the destabilizing effect of the nonlinearity f). Given υ^2, we aim to achieve the deployment with as small as possible number of leaders M.

Define characteristic functions χ_m

$$\chi_m(x) = \begin{cases} 1, & x \in [x_{m-1}, x_m] \\ 0, & x \notin [x_{m-1}, x_m] \end{cases}, m = 1, \dots, M. \qquad (2.12)$$

Then the closed-loop system (2.7), (2.11) can be considered as a discretization in the spatial variable $x \in [0, L]$ of the heat equation

$$\begin{aligned} & e_t = \upsilon^2 e_{xx} + \rho(e, t)e + \sum_{m=1}^{M} \chi_m(x)\bar{u}^m(t), \\ & \qquad\qquad x \in (0, L), \ t \geq t_0, \\ & \bar{u}^m(t) = \begin{cases} -Kq(e(\hat{x}^m, s_k^m)), & t \in [s_k^m + \eta_k^m, s_{k+1}^m + \eta_{k+1}^m), \\ 0, & t \leq t_0, \end{cases} \end{aligned} \qquad (2.13)$$

where $\hat{x}^m = 0.5(x_m - x_{m-1})$, under the Neumann boundary conditions

$$e_x(0, t) = e_x(L, t) = 0. \qquad (2.14)$$

Note that (2.3) with $e_0 = e_2$ and $e_{N+1} = e_{N-1}$ corresponds to spatial discretization under the Neumann boundary conditions. The initial condition $e(\cdot, t_0)$ is determined by the difference between the initial agents' positions and their target positions on the curve Γ. Error system (2.13) with $K = 0$ under the Neumann boundary conditions is unstable even for $\rho = 0$ (having constant solutions). Thus, K stabilizes the system compensating its nonlinearity.

Remark 2.1. For open curves, spatial discretization under the Neumann boundary conditions allows moving boundary agents with $i = 1$ and $i = N$ and recover their dynamics given by

(2.1) (as opposed to the commonly used for deployment Dirichlet boundary conditions (Meurer & Krstic, 2011), that impose immobility on the boundary agents). In Wei et al. (2019), for the case of open curve and $f_i = 0$ the following boundary conditions that correspond to boundary control were suggested

$$e_t(0,t) = -\kappa e(0,t),\ \ e_t(L,t) = -\kappa e(L,t) \tag{2.15}$$

with some $\kappa > 0$. Note that in the nonlinear case, an additional term "ρe" would be added to the right-hand side of (2.15) that may lead to instability. Moreover, as mentioned in Wei et al. (2019), even for $\rho = 0$, it is difficult to show robustness of this controller with respect to small delay. Finally periodic boundary conditions are appropriate for deployment on the closed smooth curves only (Wei et al., 2019), whereas the present controller that employs Neumann boundary conditions allows to deploy on both open and closed curves.

Well-posedness of (2.13), (2.14) can be proved similar to Fridman and Blighovsky (2012) and Fridman and Bar Am (2013). We can order all $s_k^m + \eta_k^m,\ k = 0, 1, \dots,\ m = 1, \dots, M$ as $t_0, t_1, \dots$. Note that $\bar{u}^m(t) \equiv \bar{u}^m(t_k - \eta_k)$ for all $t \in [t_k, t_{k+1})$. We will use the step method for solution of time-delay systems (see e.g. Chapter 1 of Fridman, 2014). For $t \in [t_0, t_1]$ we consider

$$e_t = \upsilon^2 e_{xx} + \rho(e,t)e + \sum_{m=1}^{M} \chi_m(x)\bar{u}^m(t_0 - \eta_0). \tag{2.16}$$

Let $\mathcal{H} = L^2(0,L)$ be a Hilbert space with the inner product $\langle\cdot,\cdot\rangle$ and induced norm $\|\cdot\|_{L^2}$. We define an unbounded linear operator $\mathcal{A} : \mathcal{D}(\mathcal{A}) \subset \mathcal{H} \to \mathcal{H}$ as follows:

$$\begin{cases} \mathcal{A}\zeta = \upsilon^2\zeta'',\ \forall \zeta \in \mathcal{D}(\mathcal{A}), \\ \mathcal{D}(\mathcal{A}) = \{\zeta \in \mathcal{H}^2(0,L) : \zeta_x(0) = \zeta_x(L) = 0\}. \end{cases} \tag{2.17}$$

It is well-known that $\mathcal{A}$ is a sectorial operator, and $\mathcal{A}$ generates an analytic semigroup (Pazy, 1983). The nonlinear term $F : \mathcal{H}^1(0,L) \times [t_0, t_1] \to L^2(0,L)$ is defined on functions $\zeta(\cdot,t)$ according to

$$F(\zeta,t) = \rho(\zeta,t)\zeta + \sum_{m=1}^{M} \chi_m(x)\bar{u}^m(t_0 - \eta_0). \tag{2.18}$$

System (2.16), (2.14) can be written as an evolution equation in $\mathcal{H}$:

$$\dot{\zeta}(t) = \mathcal{A}\zeta(t) + F(\zeta(t),t), \quad t \geq t_0. \tag{2.19}$$

A strong solution of (2.19) on $[t_0, T]$ is a function

$$\zeta \in L^2((t_0,T); \mathcal{D}(\mathcal{A})) \cap C([t_0,T]; \mathcal{H}^1(0,L)), \tag{2.20}$$

such that $\dot{\zeta} \in L^2((t_0,T); L^2(0,L))$ and (2.19) holds almost everywhere on $[t_0, T]$.

Since the function f is of class C^2, the nonlinear term F is locally Lipschitz continuous, that is, there exists a positive constant $l(\mu)$ such that the following inequality

$$\|F(\zeta^1,t^1) - F(\zeta^2,t^2)\|_{L^2} \leq l(\mu)\left[|t^1 - t^2| + \|(\zeta^1 - \zeta^2)\|_{L^2}\right]$$

holds for $t^1, t^2 \in [t_0, t_1]$ and $\zeta^1, \zeta^2 \in L^2(0,L)$ with $\|\zeta^i\|_{L^2} \leq \mu$ and $|t^i| \leq \mu$ (i = 1, 2). Moreover, since $|\rho| \leq \rho_1$ and $\bar{u}^m(t_0)$ is constant, the following holds with some $c > 0$:

$$\|F(\zeta,t)\|_{L^2} \leq c\left[1 + \|\zeta\|_{L^2}\right].$$

Then, by Theorem 3.3.3 of Henry (1981), system (2.16), (2.14) has a unique strong solution for the initial condition $\zeta(t_0) = e(\cdot,t_0) \in \mathcal{H}^1(0,L)$ and all $t \in [t_0, t_1]$ with $\zeta(t_1) \in \mathcal{H}^1(0,L)$. By considering next $t \in [t_k, t_{k+1}),\ k = 1, 2, \dots$ we conclude that (2.13), (2.14) has a unique strong solution for all $t \geq t_0$. Similarly, by Theorem 6.1.5 of Pazy (1983) for $e(\cdot,t_0) \in \mathcal{D}(\mathcal{A})$ there exists a unique classical solution $\zeta \in C([t_0,\infty); \mathcal{H}^1(0,L))$ such that $\zeta \in C^1([t_k, t_{k+1}); L^2(0,L))$ for all $k = 0, 1, \dots$ and $\zeta(t) \in \mathcal{D}(\mathcal{A})$ for all $t \geq t_0$.

2.3. ISS analysis of the closed-loop heat equation

By using the time-delay approach to networked control systems (see Chapter 7 of Fridman, 2014), denote

$$\tau^m(t) = t - s_k^m,\ \ t \in [s_k^m + \eta_k^m, s_{k+1}^m + \eta_{k+1}^m),\ \ k = 0, 1, \dots$$

where $\tau^m(t) \leq \tau_M\ \forall m = 1, \dots, M$ and τ_M is the sum of maximum transmission interval and maximum allowable delay. Then the controller (2.11) can be presented as

$$\begin{aligned} &\bar{u}_i(t) = e_{i_m}(t - \tau^m(t)) + w_m(t), \quad t \geq t_0, \\ &w_m(t) = q(e_{i_m}(t - \tau^m(t))) - e_{i_m}(t - \tau^m(t)) \end{aligned} \tag{2.21}$$

with

$$|w_m(t)| \leq \Delta_q, \quad \forall t \geq t_0. \tag{2.22}$$

Hence (2.13) can be rewritten as

$$e_t = \upsilon^2 e_{xx} + \rho e - K\sum_{m=1}^{M} \chi_m\left[e(\hat{x}_m, t - \tau^m(t)) + w_m(t)\right], \quad x \in (0,L),\ t \geq t_0. \tag{2.23}$$

Following Section 5.4 of Fridman (2014), for the ISS analysis we consider the initial condition for (2.23), (2.14) as

$$e(\cdot,t) \equiv e(\cdot,t_0) \in \mathcal{H}^1(0,L), \quad t < t_0. \tag{2.24}$$

Note that similarly to Bar Am and Fridman (2014), heat equation (2.23) may be considered as a system with spatially and time varying delay $\tau(x,t) = \sum_{m=1}^{M} \chi_m(x)\tau^m(t)$, which is upper-bounded by τ_M. In Bar Am and Fridman (2014) the direct Lyapunov–Krasovskii method was applied, where the stability analysis was the same as for identical delays $\tau(t) = \tau^1(t) = \dots = \tau^M(t)$. In this paper, due to application of Halanay's inequality, the stability analysis for the case of different $\tau^1(t), \dots, \tau^M(t)$ becomes more challenging. Note also that the quantization error $w_m(t)$ is discontinuous in time, whereas Halanay's inequality is applicable to continuous in time disturbances. Since (2.22) yields

$$\sum_{m=1}^{M} \int_{x_{m-1}}^{x_m} |w_m(t)|^2 dx \leq \Delta_q^2 L, \tag{2.25}$$

we will apply Halanay's inequality with the continuous function $w(t) \equiv \Delta_q^2 L$.

In order to derive the ISS conditions for (2.23) we employ Lyapunov functional of the form

$$V(t) = V_1(t) + V_s(t) + V_r(t),\ \ t \in [t_k, t_{k+1}),\ \ k = 0, 1, 2, \dots \tag{2.26}$$

where $V_1(t)$ is given by

$$V_1(t) = \int_0^L \left[p_1 e^2 + p_3 \upsilon^2 e_x^2\right] dx, \quad p_1, p_3 > 0 \tag{2.27}$$

and

$$V_s(t) = s\int_0^L \int_{t-\tau_M}^{t} e^{2\alpha_0(s-t)} e^2(x,s) ds\, dx, \tag{2.28}$$

$$V_r(t) = r\tau_M \int_0^L \int_{t-\tau_M}^{t} e^{2\alpha_0(s-t)} (\tau_M + s - t) e_s^2(x,s) ds\, dx$$

with some scalars $s, r \geq 0$. Here, V_s and V_r treat time-delay terms. For the strong solution of (2.23) and (2.14), the functional V is well-defined and continuous.

Theorem 2.1. *Consider the error Eq. (2.23) under the Neumann boundary conditions (2.14) initialized by (2.24) with the bounds*

τ_M, ρ_1 and Δ_q. Given $\alpha_0 > \alpha_1 > 0$, $\upsilon^2, K > \rho_1$ let there exist γ, q and positive p_1, p_2, p_3, s, r that satisfy the LMIs

$$R = \begin{bmatrix} r & q \\ * & r \end{bmatrix} \geq 0, \tag{2.29}$$

$$p_2 - \alpha_0 p_3 \geq 0, \tag{2.30}$$

and

$$\Xi_{|\rho=\pm\rho_1} = \begin{bmatrix} \xi_{11} & \xi_{12} & \xi_{13} & s\exp(-2\alpha_0\tau_M) & Kp_2 & -Kp_2 \\ * & \xi_{22} & Kp_3 & 0 & Kp_3 & -Kp_3 \\ * & * & \xi_{33} & \xi_{34} & 0 & 0 \\ * & * & * & \xi_{44} & 0 & 0 \\ * & * & * & * & \xi_{55} & 0 \\ * & * & * & * & * & -\gamma^2 \end{bmatrix} \leq 0, \tag{2.31}$$

where $\alpha_M = \frac{\alpha_1}{M}$, $\Delta = \frac{L}{M}$ and

$$\xi_{11} = 2\alpha_0 p_1 + 2p_2(\rho - K) + s\,(1 - \exp(-2\alpha_0\tau_M)) - 2\alpha_M p_1,$$

$$\xi_{12} = p_1 - p_2 + p_3(\rho - K),$$

$$\xi_{13} = s\exp(-2\alpha_0\tau_M) + Kp_2 + 2\alpha_M p_1,$$

$$\xi_{22} = \tau_M^2 r - 2p_3,$$

$$\xi_{33} = -(r+s)\exp(-2\alpha_0\tau_M) - 2\alpha_M p_1,$$

$$\xi_{34} = -(q+s)\exp(-2\alpha_0\tau_M),$$

$$\xi_{44} = -(r+s)\exp(-2\alpha_0\tau_M),$$

$$\xi_{55} = -2\alpha_M p_3 \upsilon^2(\pi^2/\Delta^2).$$

Then (1.3) holds for V defined by (2.26) on the strong solution of (2.23) and (2.14), where $\varepsilon = 2(\alpha_0 - \alpha_1)$ and $\alpha > 0$ is a unique positive solution of $\alpha = \alpha_0 - \alpha_1\exp(2\alpha\tau_M)$. Thus, (2.23) is ISS, i.e. there exist $c_0 > 0$ and $\gamma_0 > 0$ such that for all $t \geq t_0$

$$\begin{aligned} &\tfrac{1}{L+1}\max_{x\in[0,L]} e^2(x,t) \leq \|e(\cdot,t)\|^2_{\mathcal{H}^1} \\ &\leq c_0\exp\big(-2\alpha(t-t_0)\big)\|e(\cdot,t_0)\|^2_{\mathcal{H}^1} + \gamma_0\Delta_q^2 L. \end{aligned} \tag{2.32}$$

Moreover, if the strict inequalities (2.29), (2.30) and (2.31) are feasible with $\alpha_0 = \alpha_1 > 0$, then the error system (2.23), (2.14) is ISS with a small enough decay rate.

Proof. Denote

$$\nu_1 = e(x,t) - e(x, t - \tau^m(t)), \tag{2.33}$$

$$\nu_2 = e(x, t - \tau^m(t)) - e(x, t - \tau_M).$$

By employing the relations

$$e(x, t - \tau^m(t)) = e(x,t) - \nu_1(x,t), \tag{2.34}$$

$$e(\hat{x}_m, t) = e(x,t) - \int_{\hat{x}_m}^{x} e_\zeta(\zeta, t)d\zeta,$$

the error system can be represented as

$$\begin{aligned} e_t &= \upsilon^2 e_{xx} + (\rho - K)e \\ &+ K\sum_{m=1}^{M}\chi_m\left[\nu_1 + \int_{\hat{x}_m}^{x} e_\zeta(\zeta, t - \tau^m(t))d\zeta - w_m(t)\right]. \end{aligned} \tag{2.35}$$

For the strong solution of (2.19), the functional $V(t)$ given by (2.26) is well-defined and absolutely continuous. We have almost for all $t \geq t_0$

$$\begin{aligned} &\dot{V}_1(t) + 2\alpha_0 V_1(t) = \\ &\quad 2\int_0^L \left[p_1 e e_t + \upsilon^2 p_3 e_x e_{xt} + \alpha_0 p_1 e^2 + \alpha_0\upsilon^2 p_3 e_x^2\right]dx. \end{aligned}$$

Note that the derivative e_{xt} is defined in the distributional sense, where $e_{xt} = e_{tx}$ almost for all x and t (cf. Remark A.1 of Fridman & Bar Am, 2013). We further apply the descriptor method (Fridman & Blighovsky, 2012), where the right-hand side of the following expression

$$\begin{aligned} 0 \equiv\ & 2\sum_{m=1}^{M}\int_{x_{m-1}}^{x_m}[p_2 e + p_3 e_t] \\ &\times\Big[-e_t + \upsilon^2 e_{xx} + (\rho - K)e \\ &+ K\chi_m\left(\nu_1 + \int_{\hat{x}_m}^{x} e_\zeta(\zeta, t - \tau^m(t))d\zeta - w_m(t)\right)\Big]dx, \end{aligned}$$

with some constant $p_2 > 0$ is added to $\dot{V}_1$. Integrating by parts, and taking into account the boundary conditions (2.14) we have

$$2\int_0^L (p_2 e + p_3 e_t)e_{xx}dx = -2\int_0^L (p_2 e_x^2 + p_3 e_x e_{xt})dx$$

and arrive at

$$\begin{aligned} \dot{V}_1(t) \quad &+2\alpha_0 V_1(t) = 2\int_0^L \Big\{ (p_1 - p_2)e e_t - p_3 e_t^2 \\ &+ \upsilon^2(\alpha_0 p_3 - p_2)e_x^2 + \alpha_0 p_1 e^2 \Big\} dx \\ &+ 2\int_0^L [p_2 e + p_3 e_t](\rho - K)e\,dx \\ &+ 2K\sum_{m=1}^{M}\int_{x_{m-1}}^{x_m}[p_2 e + p_3 e_t]\times \\ &\Big[\nu_1 + \int_{\hat{x}_m}^{x} e_\zeta(\zeta, t - \tau^m(t))d\zeta - w_m(t)\Big]dx. \end{aligned} \tag{2.36}$$

By differentiating V_s and V_r we have

$$\dot{V}_s + 2\alpha_0 V_s = s\sum_{m=1}^{M}\int_{x_{m-1}}^{x_m}\left(e^2(x,t) - e^{-2\alpha_0\tau_M}e^2(x, t-\tau_M)\right)dx \tag{2.37}$$

with $e^2(x, t-\tau_M) = [e(x,t) - \nu_1 - \nu_2]^2$ and

$$\begin{aligned} \dot{V}_r + 2\alpha_0 V_r \quad &\leq \tau_M^2 r\sum_{m=1}^{M}\int_{x_{m-1}}^{x_m} e_t^2(x,t)dx \\ &- \tau_M r e^{-2\alpha_0\tau_M}\sum_{m=1}^{M}\int_{x_{m-1}}^{x_m}\int_{t-\tau_M}^{t} e_s^2(x,s)ds\,dx. \end{aligned} \tag{2.38}$$

Note that in (2.38) we used the inequality

$$-\int_{t-\tau_M}^{t} e^{-2\alpha_0(s-t)}e_s^2(x,s)ds \leq -e^{-2\alpha_0\tau_M}\int_{t-\tau_M}^{t} e_s^2(x,s)ds.$$

Then, under (2.29) by Lemma 3.4 of Fridman (2014) we find

$$-\tau_M r\sum_{m=1}^{M}\int_{x_{m-1}}^{x_m}\int_{t-\tau_M}^{t} e_s^2 ds\,dx \leq -\sum_{m=1}^{M}\int_{x_{m-1}}^{x_m}[\nu_1\ \nu_2]R[\nu_1\ \nu_2]^T dx. \tag{2.39}$$

We will further apply the generalized Halanay's inequality (1.3) with continuous $w(t) \equiv \Delta_q^2 L$ and some $0 < \alpha_1 < \alpha_0$. Note that

$$\begin{aligned} &\sup_{-\tau_M\leq\theta\leq 0} V(t+\theta) \geq \frac{1}{M}\sum_{m=1}^{M}\sup_{-\tau_M\leq\theta\leq 0} V_1(t+\theta) \\ &\geq \frac{1}{M}\sum_{m=1}^{M} V_1(t - \tau^m(t))dx. \end{aligned} \tag{2.40}$$

Then, employing (2.25), we have

$$\begin{aligned} W &\triangleq \dot V(t)+2\alpha_0 V(t)-2\alpha_1 \sup_{-\tau_M\le\theta\le 0} V(t+\theta) \\ &\quad -\gamma^2\Delta_q^2 L \\ &\le \dot V(t)+2\alpha_0 V(t)-\gamma^2\sum_{m=1}^{M}\int_{x_{m-1}}^{x_m}|w_m(t)|^2dx \\ &-2\alpha_M\sum_{m=1}^{M}\int_{x_{m-1}}^{x_m}\big[p_1 e^2(x,t-\tau^m(t)) \\ &+p_3\upsilon^2 e_x^2(x,t-\tau^m(t))\big]dx, \qquad \alpha_M=\frac{\alpha_1}{M}. \end{aligned} \tag{2.41}$$

By Wirtinger's inequality (1.1) we have

$$\begin{aligned} &\int_{x_{m-1}}^{x_m} e_x^2(x,t-\tau^m(t))dx = \\ &\int_{x_{m-1}}^{\hat x_m} e_x^2(x,t-\tau^m(t))dx+\int_{\hat x_m}^{x_m} e_x^2(x,t-\tau^m(t))dx \\ &\ge \frac{\pi^2}{\Delta^2}\Big[\int_{x_{m-1}}^{\hat x_m}[e(x,t-\tau^m(t))-e(\hat x_m,t-\tau^m(t))]^2dx \\ &\quad +\int_{\hat x_m}^{x_m}[e(x,t-\tau^m(t))-e(\hat x_m,t-\tau^m(t))]^2dx\Big] \\ &\ge \frac{\pi^2}{\Delta^2}\int_{x_{m-1}}^{x_m}[e(x,t-\tau^m(t))-e(\hat x_m,t-\tau^m(t))]^2dx \\ &= \frac{\pi^2}{\Delta^2}\int_{x_{m-1}}^{x_m}\Big(\int_{\hat x_m}^{x} e_\xi(\xi,t-\tau^m(t))d\xi\Big)^2dx. \end{aligned} \tag{2.42}$$

Denote

$$\eta_1=[e\ e_t\ \nu_1\ \nu_2\ \int_{\hat x_m}^{x} e_\xi(\xi,t-\tau^m(t))d\xi\ \ w_m(t)].$$

By taking into account (2.37)–(2.39), (2.41) and (2.42), we arrive at

$$\begin{aligned} &W\le \dot V(t)+2\alpha_0 V(t)-\gamma^2\textstyle\sum_{m=1}^{M}\int_{x_{m-1}}^{x_m}|w_m(t)|^2dx \\ &-2\alpha_M\textstyle\sum_{m=1}^{M}\int_{x_{m-1}}^{x_m}[p_1(e-\nu_1)^2+p_3\upsilon^2 e_x^2(x,t-\tau^m(t))]dx \\ &\le -2\upsilon^2(p_2-\alpha_0 p_3)\int_0^L e_x^2dx+\textstyle\sum_{m=1}^{M}\int_{x_{m-1}}^{x_m}\eta_1\Xi\eta_1^T dx\le 0 \end{aligned}$$

if $\Xi\le 0$, where Ξ is given by (2.31). Note that Ξ is affine in ρ. Thus, it is sufficient to verify (2.31) in the vertices $\pm\rho_1$.

Due to Halanay's inequality, (1.3) holds under (2.29)–(2.31) implying (2.32) due to Sobolev's inequality (1.2) with $C=1$. The feasibility of strict LMIs with $\alpha_0=\alpha_1=0$ implies their feasibility with a slightly larger $\bar\alpha_0=\alpha_0+\delta>0$, where $\delta>0$ is small, that completes the proof.

Remark 2.2. Differently from the existing works on distributed sampled-data control under point measurements (Fridman & Blighovsky, 2012; Terushkin & Fridman, 2019; Wei et al., 2019), we consider the point measurements (2.21) under the different delays $\tau^m(t)$ that leads to more restrictive conditions via Halanay's inequality with $\alpha_M=\frac{\alpha_1}{M}$ instead of α_1 for equal delays $\tau^1=\cdots=\tau^M$. Note that still it is easier to satisfy the resulting conditions for $M\gg 1$ than for $M=1$ since the main stabilizing term with the coefficient $-\frac{\alpha_1}{M}p_3\upsilon^2$ in (2.41) after application of Wirtinger's inequality in (2.42) leads to

$$\psi_{55}=-\frac{\alpha_1}{M}p_3\upsilon^2\frac{\pi}{\Delta^2}=-\alpha_1 M p_3\upsilon^2\frac{\pi}{L^2}\underset{M\to\infty}{\Longrightarrow}-\infty.$$

Remark 2.3. Given M and $M\alpha_0\ge\alpha_M>0$, LMIs (2.29), (2.30) and (2.31) are always feasible for $K>\rho_1+\alpha_0-\alpha_M$ and large enough υ^2, γ^2 and τ_M^{-1}. Indeed, let us choose $s=q=0$, $p_1=p_2\ge\alpha_0$ and $p_3=1$. For $\tau_M\to 0$, $\gamma^2\to\infty$ and $\upsilon^2\to\infty$ these LMIs are feasible if

$$\Psi_0=\begin{bmatrix} 2p_1(\alpha_0-\alpha_M+\rho-K) & \rho-K & (K+2\alpha_M)p_1 \\ * & -2 & K \\ * & * & -r-2\alpha_M p_1\end{bmatrix}<0.$$

We choose p_1 such that $2p_1(\alpha_0-\alpha_M+\rho_1-K)+0.5(\rho_1+K)^2<0$. Then, by Schur complement, $\Psi_0<0$ for large enough $r>0$. With the chosen p_1 and r, LMIs (2.29), (2.30) and (2.31) hold for large enough υ^2, γ^2 and τ_M^{-1}.

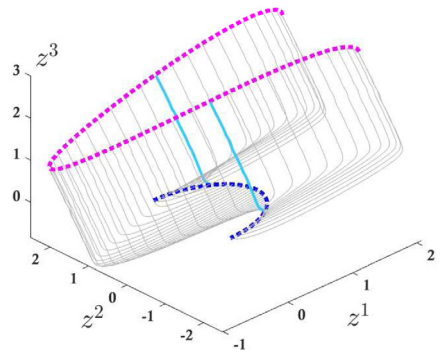

Fig. 2. Open curve: deployment of $N=49$ agents from Γ_0 (blue) to Γ (pink), with $M=2$ leaders (trajectories in cyan). (For interpretation of the references to color in this figure legend, the reader is referred to the web version of this article.)

Remark 2.4. The PDE-based approach to MAS leads to novel control laws ($\bar u_i(t)$-term in (2.4), (2.11) in the present paper). One can directly derive LMI stability conditions for the N-dimensional ODE system (2.1) with an appropriate control law. Then, there will be $N\times N$ decision variables (instead of the scalar ones in our approach). For large N, it may be difficult to verify the LMIs feasibility in Matlab. Moreover, new LMIs should be derived for a new value of N. Therefore, the PDE-based approach gives new control laws and simplified lower-order LMI conditions that are appropriate for all large enough N.

2.4. Numerical simulations: first-order MAS

In the sequel, we validate the proposed control for agents governed by the first-order dynamics in $\mathbb{R}^3$. Throughout the simulations we consider a group of $N=49$ agents, whereas in all the figures of the deployment, the pink dashed lines are the desired positions, and the blue dashed lines are the initial positions.

Consider a group of N agents, governed by (2.1) with a nonlinear function $f^j=\sin(z^j)$ with $j\in\{1,2,3\}$, where $\rho_1=1$ in (2.2). Our objective is deployment from initial positions on $\Gamma_0(x)$, parameterized by $x\in[0,\pi]$, onto desired positions of open curve $\Gamma(x)$ ($x\in[0,\pi]$) defined as (see Fig. 2)

$$\begin{aligned} &\Gamma_0(ih)=[\sin(ih),\cos(ih),0],\quad h=\frac{\pi}{N},\ i=1,\dots,N \\ &\Gamma(ih)=[\sin(ih)+2\cos(2ih),\cos(ih)+2\sin(ih),2+\cos(2ih)], \end{aligned} \tag{2.43}$$

or from initial positions on $\Gamma_0(x)$ onto desired positions of closed curve $\Gamma(x)$ with $x\in[0,2\pi]$ given by (see Fig. 3)

$$\begin{aligned} &\Gamma_0(ih)=[\sin(ih),\cos(ih),0],\quad h=\frac{2\pi}{N},\ i=1,\dots,N \\ &\Gamma(ih)=\Big[0.8\sin^3(ih),0.015\Big(12\cos(ih)-6\cos(2ih) \\ &\quad -3\cos(3ih)-\cos(4ih)\Big),3.5\Big]. \end{aligned} \tag{2.44}$$

We design a controller with the gains

$$\upsilon^2=4,\quad K=2. \tag{2.45}$$

LMIs of Theorem 2.1 are verified in both vertices $\rho=\pm\rho_1=\pm 1$. By verifying the LMIs of Theorem 2.1 with $\alpha_0=\alpha_1=0.4$, we find

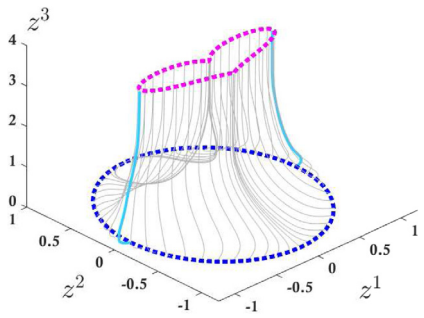

Fig. 3. Closed curve: deployment of $N = 49$ agents from Γ_0 (blue) to Γ (pink), with $M = 2$ leaders (trajectories in cyan). (For interpretation of the references to color in this figure legend, the reader is referred to the web version of this article.)

that the closed-loop system led by two ($M = 2$) agents placed in the middle of the sampling intervals of the length Δ ($\Delta = \frac{\pi}{2}$ in the case of open curve and $\Delta = \pi$ in the case of closed curve) is ISS provided $\tau_M \leq 0.3$. Note that increasing υ^2 till 6, results in 1 leader being sufficient for deployment if $\tau_M \leq 0.24$.

We further show simulations of the deployment for $M = 2$, $\tau_M = 0.3$, where the network induced delays are bounded by $\eta_k^m \leq 0.02$, and quantization error is bounded by $\Delta_q = 0.01$. The agents are divided into two groups: (1) leader $z_{i_1} = z_{13}$ amidst agents $z_1, \ldots, z_{24}$ and (2) leader $z_{i_2} = z_{37}$ amidst agents $z_{25}, \ldots, z_{49}$. Figs. 2–3 depict the transitions of a system driven by two leaders from initial (marked blue) to final (marked pink) open or closed curves, given by (2.43)–(2.44). Trajectories of the leaders are shown in cyan, whereas the trajectories of the followers are shown in gray. From simulations, the ISS is preserved till larger $\tau_M = 1.6$, which illustrates the conservatism of LMIs.

3. Deployment of the second-order MAS

3.1. Problem formulation and controller design

Consider now a group of N agents, governed by the second-order dynamics, that can move in space $\mathbb{R}^n, n \in \{2, 3\}$. The dynamics of each agent is given by

$$\begin{aligned} &\ddot{z}_i^j = u_i^j + f^j(z_i, t), \quad j \in \{1, \ldots, n\}, \quad n = 2, 3, \\ &i = 1, \ldots, N, \quad t \geq t_0, \end{aligned} \tag{3.1}$$

where the nonlinearities f^j are of class C^2. Here $z_i^j \in \mathbb{R}$ and u_i^j are components of the position and control for ith agent, respectively. For brevity, the super-script j will be further omitted. We assume the derivative $f_z(z, t)$ is uniformly bounded by a constant $\rho_1 > 0$ as given in (2.2).

Our aim is to deploy N agents onto a C^2 curve $\Gamma : [0, L] \longrightarrow \mathbb{R}^n$. We suppose that all assumptions of Section 2.1 hold. Additionally to (1)-(3), for the second-order MAS we assume
(4) All the agents measure their own velocity $\dot{z}_i$ with respect to the global coordinate system.

Our objective is to deploy the agents onto the desired curve Γ by exploiting $M \ll N$ leaders. We propose the following static output-feedback controller

$$\begin{aligned} u_i(t) = &\frac{\upsilon^2}{h^2}\left[z_{i+1}(t) - 2z_i(t) + z_{i-1}(t)\right] \\ &- \frac{\upsilon^2}{h^2}\left[\Gamma\big((i+1)h\big) - 2\Gamma\big(ih\big) + \Gamma\big((i-1)h\big)\right] \\ &- \beta\dot{z}_i(t) - f(\Gamma(ih), t) + \bar{u}_i(t), \quad i = 1, \ldots, N, \end{aligned} \tag{3.2}$$

where the network-based controller $\bar{u}_i$ is defined in Section 2.2 and is given by (2.11). Note that the proposed controller (3.2), (2.11) contains three gains: υ^2 which allows to reduce the number of the leaders, $\beta > 0$ which improves the convergence and $K > 0$ which compensates the destabilizing effect of the nonlinearity f. By denoting the error $e_i(t) = z_i(t) - \Gamma(ih)$ and taking into account (2.5), we can represent the closed-loop system (2.1), (3.2) as:

$$\begin{aligned} \ddot{e}_i(t) = &\frac{\upsilon^2}{h^2}\left[e_{i+1}(t) - 2e_i(t) + e_{i-1}(t)\right] \\ &- \beta e_t + \rho(e_i, t)e_i(t) + \bar{u}_i(t), \quad i = 1, \ldots, N, \end{aligned} \tag{3.3}$$

where the network-based control $\bar{u}_i(t)$ based on the measurements of M leaders is defined in Section 2.2 and is given by (2.21).

System (3.3), (2.21) can be considered as a discretization in the spatial variable of the damped wave equation

$$\begin{aligned} &e_{tt}(x, t) = \upsilon^2 e_{xx}(x, t) - \beta e_t(x, t) + \rho(e, t)e(x, t) \\ &\quad + \sum_{m=1}^{M} \chi_m(x)\bar{u}^m(t), \quad x \in (0, L), \ t \geq t_0, \\ &\bar{u}^m(t) = \begin{cases} -Kq(e(\hat{x}^m, s_k^m)), & t \in [s_k^m + \eta_k^m, s_{k+1}^m + \eta_{k+1}^m), \\ 0, & t \leq t_0, \end{cases} \end{aligned} \tag{3.4}$$

where $\chi_m(x)$ is defined by (2.12), under the Neumann boundary conditions (2.14). The initial condition $e(\cdot, t_0)$ is determined by the difference between the initial agents positions and their target positions on the curve Γ, whereas $e_t(\cdot, t_0)$ is determined by the initial agents' velocities. Due to (2.2) the inequality (2.6) holds. For the well-posedness, we present the state of (3.5), (2.14) as $\zeta(t) = [\zeta_0(t)\ \zeta_1(t)]^T = [e\ e_t(t)]^T$. Consider the Hilbert space $\mathcal{H} = \mathcal{H}^1(0, L) \times L^2(0, L)$ and $\|\zeta\|_{\mathcal{H}}^2 = \|\zeta_{0x}\|_{L^2}^2 + \|\zeta_1\|_{L^2}^2$. Denote

$$\mathcal{A} = \begin{bmatrix} 0 & I \\ \upsilon^2 \frac{\partial^2}{\partial x^2} & -\beta I \end{bmatrix}.$$

The operator $\mathcal{A}$ with the dense domain

$$\mathcal{D}(\mathcal{A}) = \Big\{ \begin{bmatrix} \zeta_0 & \zeta_1 \end{bmatrix}^T \in \mathcal{H}^2(0, L) \times \mathcal{H}^1(0, L) \ \Big| \ \zeta_{0x}(0) = \zeta_{0x}(L) = 0 \Big\}$$

generates a strongly continuous semigroup (Pazy, 1983).

We order $s_k^m + \eta_k^m$, $k = 0, 1, \ldots$, $m = 1, \ldots, M$ as $t_0, t_1, \ldots$ By employing the step method for $t \in [t_0, t_1]$, $t \in [t_1, t_2]$ and applying Theorems 6.1.2 and 6.1.5 from Pazy (1983) (see details in Terushkin & Fridman, 2019), we find that a unique mild solution exists in $C([t_0, \infty), \mathcal{H})$ for (3.5), (2.14), initialized by $[e(\cdot, t_0)\, e_t(\cdot, t_0)]^T \in \mathcal{H}$. Moreover, if $[e(\cdot, t_0)\, e_t(\cdot, t_0)]^T \in \mathcal{D}(\mathcal{A})$, then there exists a unique classical solution $\zeta \in C([t_0, \infty); \mathcal{H})$ such that $\zeta \in C^1([t_k, t_{k+1}); \mathcal{H})$ for all $k = 0, 1, \ldots$ and $\zeta(t) \in \mathcal{D}(\mathcal{A})$ for all $t \geq t_0$.

3.2. ISS analysis of the closed-loop wave equation

By employing the time-delay representation of $\bar{u}_i$ given by (2.21), we rewrite (3.4) as

$$\begin{aligned} &e_{tt}(x, t) = \upsilon^2 e_{xx}(x, t) - \beta e_t(x, t) + \rho(e, t)e(x, t) \\ &\quad - K\sum_{m=1}^{M} \chi_m \left[e(\hat{x}_m, t - \tau^m(t)) + w_m(t)\right], \\ &\beta > 0, \ x \in (0, L), \ t \geq t_0. \end{aligned} \tag{3.5}$$

We assume $\tau^m(t) \le \tau_M$, whereas w_m is subject to (2.22). Consider the following initial conditions for (3.5), (2.14):

$$e(\cdot,t) \equiv e(\cdot,t_0) \in \mathcal{H}^1(0,L), \quad t \le t_0$$

$$e_t(\cdot,t) \equiv e_t(\cdot,t_0) \in L^2(0,L). \tag{3.6}$$

For the choice of the controller gains β and K we follow Remark 3.1 of Terushkin and Fridman (2019), where larger β and $K = \rho_1 + \frac{\beta^2}{4}$ lead to a faster convergence.

In order to derive the ISS conditions for (3.5), (2.14) we employ Lyapunov functional of the form (Terushkin & Fridman, 2019)

$$V(t) = V_0(t) + V_s(t) + V_r(t), \ \ t \in [t_k, t_{k+1}), \ \ k = 0, 1, 2, \dots \tag{3.7}$$

where $V_0(t)$ is given by

$$V_0(t) = p_3 \upsilon^2 \int_0^L e_x^2 dx + \int_0^L [e \ e_t] P_0 [e \ e_t]^T dx, \tag{3.8}$$

with P_0 given by

$$P_0 = \begin{bmatrix} p_1 & p_2 \\ * & p_3 \end{bmatrix} > 0, \tag{3.9}$$

and V_s and V_r are defined by (2.28). This functional is defined on the mild solutions of (3.5), (2.14), and due to (3.9) it is positive definite with $V(t) \ge c'(\|e_x(\cdot,t)\|^2_{L^2} + \|e_t(\cdot,t)\|^2_{L^2})$ for some $c' > 0$.

Theorem 3.1. *Consider the damped wave equation (3.5) under the Neumann boundary conditions (2.14) initialized by (3.6) with the bounds τ_M, ρ_1 and Δ_q. Given $\alpha_0 > \alpha_1 > 0$, $\upsilon^2, \beta > \alpha_0$, $K = \rho_1 + \frac{\beta^2}{4}$, let there exist $\gamma, s > 0$, $r > 0$, q and p_1, p_2, p_3 that satisfy the LMIs (2.29), (3.9),*

$$p_2 - \alpha_0 p_3 \ge 0, \tag{3.10}$$

and

$$\Psi_{|\rho=\pm\rho_1} = \begin{bmatrix} \psi_{11} & \psi_{12} & \psi_{13} & \psi_{14} & Kp_2 & -2\alpha_M p_2 & -Kp_2 \\ * & \psi_{22} & Kp_2 + \tau_M^2 r & 0 & Kp_2 & 0 & -Kp_2 \\ * & * & \psi_{33} & \psi_{34} & 0 & 2\alpha_M p_2 & 0 \\ * & * & * & \psi_{44} & 0 & 0 & 0 \\ * & * & * & * & \psi_{55} & 0 & 0 \\ * & * & * & * & * & -2\alpha_M p_3 & 0 \\ * & * & * & * & * & * & -\gamma^2 \end{bmatrix} \le 0, \tag{3.11}$$

where $\alpha_M = \frac{\alpha_1}{M}$, $\Delta = \frac{L}{M}$ and

$$\psi_{11} = 2p_2(\rho - K) + 2(\alpha_0 - \alpha_M)p_1 + s(1 - \exp(-2\alpha_0\tau_M)),$$

$$\psi_{12} = p_1 + p_2(2\alpha_0 - \beta) + p_3(\rho - K),$$

$$\psi_{13} = Kp_2 + s\exp(-2\alpha_0\tau_M) + 2\alpha_M p_1,$$

$$\psi_{14} = s\exp(-2\alpha_0\tau_M), \ \ \psi_{22} = 2p_2 + 2p_3(\alpha_0 - \beta),$$

$$\psi_{33} = -(s+r)\exp(-2\alpha_0\tau_M) - 2\alpha_M p_1,$$

$$\psi_{34} = -(s+q)\exp(-2\alpha_0\tau_M),$$

$$\psi_{44} = -(s+r)\exp(-2\alpha_0\tau_M), \ \ \psi_{55} = -2\alpha_M p_3 \upsilon^2(\pi^2/\Delta^2).$$

Then (1.3) holds for V defined by (3.7) on the mild solutions of (3.5) and (2.14), where $\varepsilon = 2(\alpha_0 - \alpha_1)$ and $\alpha > 0$ is a unique positive solution of $\alpha = \alpha_0 - \alpha_1\exp(2\alpha\tau_M)$. Thus, (3.5), (2.14) is ISS, i.e. there exist $c_0 > 0$ and $\gamma_0 > 0$ such that for all $t \ge t_0$

$$\begin{aligned} &\tfrac{1}{L+1}\max_{x\in[0,L]} e^2(x,t) \le \left[\|e(\cdot,t)\|^2_{\mathcal{H}^1} + \|e_t(\cdot,t)\|^2_{L^2}\right] \\ &\le c_0 \exp\big(-2\alpha(t-t_0)\big)\left[\|e(\cdot,t_0)\|^2_{\mathcal{H}^1} + \|e_t(\cdot,t_0)\|^2_{L^2}\right] \\ &\quad + \gamma_0 \Delta_q^2 L. \end{aligned} \tag{3.12}$$

Moreover, if the strict inequalities (3.9)–(3.11) are feasible with $\alpha_0 = \alpha_1 > 0$, then the error system (3.5), (2.14) is ISS with a small enough decay rate.

Proof. By employing (2.33) and (2.34), the error dynamics can be represented as

$$\begin{aligned} e_{tt} &= \upsilon^2 e_{xx} - \beta e_t + (\rho - K)e \\ &\quad + K\sum_{m=1}^{M} \chi_m \left[\nu_1 + \int_{\hat{x}_m}^{x} e_\zeta(\zeta, t - \tau^m(t))d\zeta - w_m(t)\right]. \end{aligned} \tag{3.13}$$

As in Fridman (2013), we consider first $[e(\cdot,t_0), \ e_t(\cdot,t_0)]^T \in \mathcal{D}(\mathcal{A})$. Then we can differentiate $V(t)$ defined by (3.7) along the classical solutions of the wave equation. We proceed with differentiation of (3.7) along (3.5). Note that integration by parts and substitution of boundary conditions leads to

$$\int_0^L (p_2 e + p_3 e_t)\, e_{xx} dx = -\int_0^L \left(p_2 e_x^2 + p_3 e_x e_{xt}\right) dx.$$

Then

$$\begin{aligned} \dot{V}_0 + 2\alpha_0 V_0 &\le 2\upsilon^2(\alpha_0 p_3 - p_2)\int_0^L e_x^2 dx \\ &+ \int_0^L [e \ e_t] G [e \ e_t]^T dx + 2\sum_{m=1}^{M}\int_{x_{m-1}}^{x_m} K(p_2 e + p_3 e_t) \\ &\times \left[\nu_1 + \int_{\hat{x}_m}^{x} e_\zeta(\zeta, t - \tau^m(t))d\zeta - w_m(t)\right] dx \end{aligned}$$

where

$$G \triangleq \begin{bmatrix} 2p_2(\rho - K) + 2\alpha_0 p_1 & p_1 + p_2(2\alpha_0 - \beta) + p_3(\rho - K) \\ * & 2p_2 + 2p_3(\alpha_0 - \beta) \end{bmatrix}.$$

We will further apply the generalized Halanay's inequality (1.3) for some $0 < \alpha_1 < \alpha_0$. Taking into account (2.40) with V_1 changed by V_0 and (2.25), we have

$$\begin{aligned} W &\triangleq \dot{V}(t) + 2\alpha_0 V(t) - 2\alpha_1 \sup_{-\tau_M \le \theta \le 0} V(t+\theta) - \gamma^2 \Delta_q^2 L \\ &\le \dot{V}(t) + 2\alpha_0 V(t) - 2\alpha_M p_3 \upsilon^2 \sum_{m=1}^{M}\int_{x_{m-1}}^{x_m} e_x^2(x, t - \tau^m(t))dx \\ &- \gamma^2 \sum_{m=1}^{M}\int_{x_{m-1}}^{x_m} |w_m(t)|^2 dx, \quad \alpha_M = \frac{\alpha_1}{M}. \end{aligned} \tag{3.14}$$

Let ν_1 and ν_2 be given by (2.33). Denote

$$\eta = [e \ e_t \ \nu_1 \ \nu_2 \int_{\hat{x}_m}^{x} e_\xi(\xi, t - \tau^m(t))d\xi \ e_t(x, t - \tau^m(t)) \ w_m(t)].$$

Then, (3.10), (3.14), (2.37)–(2.39) and (2.42) yield

$$W \le 2\upsilon^2(\alpha_0 p_3 - p_2)\int_0^L e_x^2 dx + \sum_{m=1}^{M}\int_{x_{m-1}}^{x_m} \eta \Psi \eta^T dx \le 0$$

if $\Psi \le 0$, where Ψ is given by (3.11). Note that Ψ is affine in ρ. Thus, it is sufficient to verify (3.11) in the vertices $\pm\rho_1$. The rest of the proof is similar to Theorem 2.1.

Remark 3.1. Consider $K = \rho_1 + \frac{\beta^2}{4}$. Assume that the following LMIs hold: (3.9) and $\Psi^0_{|\rho=\pm\rho_1} < 0$, where

$$\Psi^0 \triangleq \begin{bmatrix} 2p_2(\rho - K) + 2\alpha_0 p_1 & \psi_{12} \\ * & 2p_2 + 2p_3(\alpha_0 - \beta) \end{bmatrix}.$$

Then, by arguments of Theorem 3.1 in Terushkin and Fridman (2019), the LMIs (2.29), (3.9), (3.10) and (3.11) are feasible for any

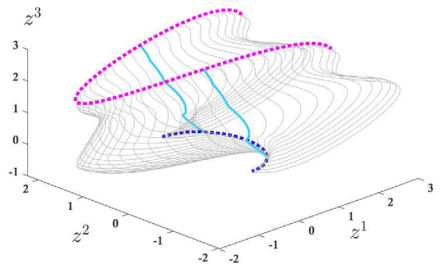

Fig. 4. Deployment of $N = 49$ agents from Γ_0 (blue) to Γ (pink), with $M = 2$ leaders (trajectories in cyan). (For interpretation of the references to color in this figure legend, the reader is referred to the web version of this article.)

$\alpha_1 < \alpha_0$ and large enough υ^2, γ^2 and τ_M^{-1}. Note that $\Psi^0_{|\rho=\rho_1} < 0$ and $P_0 > 0$ are always feasible, whereas $\Psi^0_{|\rho=\pm\rho_1} < 0$ and $P_0 > 0$ are feasible for small enough ρ_1.

3.3. Numerical simulations: second-order MAS

We validate the proposed control approach in a simulation with $N = 49$ agents in $\mathbb{R}^3$. Consider a group of N agents, governed by (3.1) with a linear $f^j = z^j$ with $j \in \{1, 2, 3\}$, where $\rho_1 = 1$ in (2.2). Our objective is deployment from initial positions on $\Gamma_0(x)(x \in [0, \pi])$ to desired positions on a smooth open curve $\Gamma(x)(x \in [0, \pi])$ given by (2.43). We design a controller with the gains

$$\upsilon^2 = 4.1,\ \beta = 3,\ K = 1 + \beta^2/4. \tag{3.15}$$

For the linear system, LMI (3.11) of Theorem 3.1 is verified only in one vertex $\rho = \rho_1 = 1$. We find that the LMIs of Theorem 3.1 are feasible for $M \geq 2$ leaders. By further verifying the LMIs of Theorem 3.1 with $\alpha_0 = \alpha_1 = 0.4$, we find that the system with two leaders ($M = 2$) is ISS provided $\tau_M \leq 0.52$. Note that increasing υ^2 till 5.1, results in one leader being sufficient for deployment if $\tau_M \leq 0.29$.

We further show simulations of the deployment for $M = 2$, $\tau_M = 0.52$, where the network induced delays are bounded by $\eta_k^m \leq 0.02$, and quantization error is bounded by $\Delta_q = 0.01$. As in Section 2.4, the agents are divided into two groups: (1) leader $z_{i_1} = z_{13}$ amidst agents $z_1, \ldots, z_{24}$ and (2) leader $z_{i_2} = z_{37}$ amidst agents $z_{25}, \ldots, z_{49}$. Fig. 4 depicts the transitions of a system driven by two leaders from initial (marked blue) to final (marked pink) open curves. Trajectories of the leaders are shown in cyan, whereas the trajectories of the followers are shown in gray. From simulations, the ISS is preserved till essentially larger $\tau_M = 2.1$, which illustrates the conservatism of LMI conditions.

4. Conclusions

We presented a network-based deployment of a large-scale first and second-order nonlinear MAS onto a smooth (open or closed) curve. A static output-feedback controller was designed by employing the measurements by each agent of his position with respect to the closest neighbors (and his velocity for the second-order agents) as well as the measurements of the leaders' absolute positions with respect to the curve that were sent through communication network to other agents. The proposed method can be extended in the future to locally Lipschitz nonlinearities and to constrained (e.g. due to quantization) network-based control $\bar{u}_i(t)$ that should lead to regional results (similar to Terushkin & Fridman, 2020a).

References

Bar Am, N., & Fridman, E. (2014). Network-based H_∞ filtering of parabolic systems. *Automatica*, *50*, 3139–3146.

Dunbabin, M., & Marques, L. (2012). Robots for environmental monitoring: Significant advancements and applications. *IEEE Robotics & Automation Magazine*, *19*(1), 24–39.

Freudenthaler, G., & Meurer, T. (2020). PDE-based multi-agent formation control using flatness and backstepping: Analysis, design and robot experiments. *Automatica*, *115*, Article 108897.

Fridman, E. (2013). Observers and initial state recovering for a class of hyperbolic systems via Lyapunov method. *Automatica*, *49*(7), 2250–2260.

Fridman, E. (2014). *Systems and control: Foundations and applications*, *Introduction to time-delay systems: Analysis and control*. Birkhauser.

Fridman, E., & Bar Am, N. (2013). Sampled-data distributed H_∞ control of transport reaction systems. *SIAM Journal on Control and Optimization*, *51*(2), 1500–1527.

Fridman, E., & Blighovsky, A. (2012). Robust sampled-data control of a class of semilinear parabolic systems. *Automatica*, *48*, 826–836.

Fridman, E., & Dambrine, M. (2009). Control under quantization, saturation and delay: An LMI approach. *Automatica*, *45*, 2258–2264.

Frihauf, P., & Krstic, M. (2010). Leader-enabled deployment onto planar curves: A PDE-based approach. *IEEE Transactions on Automatic Control*, *56*(8), 1791–1806.

Henry, D. (1981). *Lecture Notes in Mathematics*, *Geometric Theory of Semilinear Parabolic Equations (vol. 840)*. Springer Berlin Heidelberg.

Jie, Q., Feng, P., & Jinpeng, Q. (2015). A PDE approach to formation tracking control for multi-agent systems. In *2015 34th Chinese control conference* (pp. 7136–7141). IEEE.

Kang, W., & Fridman, E. (2019). Distributed stabilization of Korteweg–de Vries–Burgers equation in the presence of input delay. *Automatica*, *100*, 260–273.

Liberzon, D. (2003). Hybrid feedback stabilization of systems with quantized signals. *Automatica*, *39*(9), 1543–1554.

Mesbahi, M., & Egerstedt, M. (2010). *Graph theoretic methods in multiagent networks (vol. 33)*. Princeton University Press.

Meurer, T. (2012). *Control of higher–dimensional PDEs: Flatness and backstepping designs*. Springer Science & Business Media.

Meurer, T., & Krstic, M. (2011). Finite-time multi-agent deployment: A nonlinear PDE motion planning approach. *Automatica*, *47*(11), 2534–2542.

Oh, K.-K., Park, M.-C., & Ahn, H.-S. (2015). A survey of multi-agent formation control. *Automatica*, *53*, 424–440.

Olfati-Saber, R. (2006). Flocking for multi-agent dynamic systems: Algorithms and theory. *IEEE Transactions on Automatic Control*, *51*(3), 401–420.

Pazy, A. (1983). *Semigroups of linear operators and applications to partial differential equations (vol. 44)*. Springer New York.

Pilloni, A., Pisano, A., Orlov, Y., & Usai, E. (2015). Consensus-based control for a network of diffusion PDEs with boundary local interaction. *IEEE Transactions on Automatic Control*, *61*(9), 2708–2713.

Qi, J., Wang, S., Fang, J.-a., & Diagne, M. (2019). Control of multi-agent systems with input delay via PDE-based method. *Automatica*, *106*, 91–100.

Ren, W., Beard, R. W., & Atkins, E. M. (2007). Information consensus in multivehicle cooperative control. *IEEE Control Systems Magazine*, *27*(2), 71–82.

Tang, S.-X., Qi, J., & Zhang, J. (2017). Formation tracking control for multi-agent systems: A wave-equation based approach. *International Journal of Control, Automation and Systems*, *15*(6), 2704–2713.

Terushkin, M., & Fridman, E. (2019). Sampled-data observers for semilinear damped wave equations under spatially sampled state measurements. *Automatica*, *106*, 150–160.

Terushkin, M., & Fridman, E. (2020a). Network-based control of a semilinear damped beam equation under point and pointlike measurements. *Systems & Control Letters*, *136*, Article 104617.

Terushkin, M., & Fridman, E. (2020b). Network-based deployment of the second-order multi agents: A PDE approach. In *21st IFAC world congress. Berlin*.

Wei, J., Fridman, E., & Johansson, K. H. (2019). A PDE approach to deployment of mobile agents under leader relative position measurements. *Automatica*, *106*, 47–53.

Wen, L., Yu, Y., & Wang, W. (2008). Generalized Halanay inequalities for dissipativity of Volterra functional differential equations. *Journal of Mathematical Analysis and Applications*, *347*(1), 169–178.

Maria Terushkin received her M.Sc. degree in 2016, in Electrical Engineering at Tel-Aviv University, Israel, where she is currently a Ph.D. student. Her research interests include distributed-parameter systems, networked-control systems, time-delay systems.

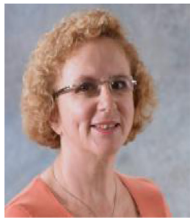

Emilia Fridman received the M.Sc. degree from Kuibyshev State University, USSR, in 1981 and the Ph.D. degree from Voronezh State University, USSR, in 1986, all in mathematics. From 1986 to 1992 she was an Assistant and Associate Professor in the Department of Mathematics at Kuibyshev Institute of Railway Engineers, USSR. Since 1993 she has been at Tel Aviv University, where she is currently Professor of Electrical Engineering-Systems. She has held visiting positions at the Weierstrass Institute for Applied Analysis and Stochastics in Berlin (Germany), INRIA in Rocquencourt (France), Ecole Centrale de Lille (France), Valenciennes University (France), Leicester University (UK), Kent University (UK), CINVESTAV (Mexico), Zhejiang University (China), St. Petersburg IPM (Russia), Melbourne University (Australia), Supelec (France), KTH (Sweden).

Her research interests include time-delay systems, networked control systems, distributed parameter systems, robust control, singular perturbations and nonlinear control. She has published more than 190 articles in international scientific journals and two monographs. She serves/served as Associate Editor in Automatica, SIAM Journal on Control and Optimization and IMA Journal of Mathematical Control and Information. In 2014 she was Nominated as a Highly Cited Researcher by Thomson ISI. Since 2018, she has been the incumbent for Chana and Heinrich Manderman Chair on System Control at Tel Aviv University. She is IEEE Fellow. She is currently a member of the IFAC Council.